P1-023

Erosion of tungsten and steel in the main chamber of ASDEX Upgrade

A. Hakola[a]*, S. Koivuranta[a], J. Likonen[a], A. Herrmann[b], H. Maier[b], M. Mayer[b], R. Neu[b,c], V. Rohde[b], ASDEX Upgrade Team

[a]*VTT, P.O. Box 1000, 02044 VTT, Finland*

[b]*Max-Planck-Institut für Plasmaphysik, Boltzmannstrasse 2, 85748 Garching, Germany*

[c]*Technische Universität München, 85747 Garching, Germany*

Abstract

We have investigated net erosion and deposition of W and P92 steel in ASDEX Upgrade during its full-W operational phase. The outer divertor and the outer midplane are the strongest net erosion region for W, with rates up to 0.12nm/s and 0.05nm/s, respectively. The eroded W is transported via the scrape-off layer plasma and predominantly deposited in the upper (20-30%) and inner divertors (40-60%). The inner midplane does not contribute significantly to the erosion-deposition balance such that the remaining W is deposited in shadowed areas of the tokamak. Steel is eroded 3-10 times faster than W but could be used at the top and inner parts of the main chamber where the erosion rate is ~0.01nm/s.

PACS: 52.40.Hf, 52.55.Fa, 68.49.Sf, 82.80.Yc

PSI-21 keywords: ASDEX-Upgrade, Erosion & Deposition, First wall, Surface analysis, Tungsten

**Corresponding author address*: VTT Reactor Physics, P. O. Box 1000, 02044 VTT, Finland

**Corresponding author e-mail*: antti.hakola@vtt.fi

Presenting author: Dr. Antti Hakola

Presenting author e-mail: antti.hakola@vtt.fi

1. Introduction

Migration of materials in the scrape-off layer (SOL) plasma of a tokamak is a high-priority research topic in the European fusion programme [1]. To fully understand the migration process, one needs information on how different plasma-facing components (PFCs) are eroded during long- and short-term plasma operations and how the eroded material is deposited at other locations, possibly forming tritium-rich co-deposited layers with plasma particles. Experimentally, the erosion and deposition processes can be investigated by installing marker probes into specific locations of the tokamak and determining the changes in the thicknesses of the markers and the compositions of the deposited layers using standard surface-analysis techniques [2].

Here we report the net erosion/deposition patterns on PFCs in different regions of ASDEX Upgrade (AUG), which presently is the only DEMO-relevant, full-W tokamak in Europe [3]. The article concentrates on the potential PFC materials tungsten [4] and EUROFER steel [5,6], which is here mostly represented by Ni.

Most of the data have been obtained from long-term exposures of marker tiles in the divertor region, where typically the strongest plasma-wall interaction processes take place [7]. Recently, however, the focus of the research has shifted to the main chamber, especially to the top parts of the vessel and to the limiters around the high-field side (inner) midplane (heat shield). In addition, marker probes have been exposed to a pre-determined number of plasma shots at the low-field side (outer) midplane, which is a noticeable net-erosion region in AUG [7]. Notice that an average AUG campaign (~3000-5000s) equals one ITER discharge (~400s) in terms of the particle fluence. However, due to larger plasma temperatures at the divertor (10 eV vs. 3 eV), the energy load and thus the expected erosion will be considerably larger in AUG than in ITER.

2. Experiments

2.1 Marker tiles in 2007-2013

Marker tiles were exposed to plasmas during the 2007, 2008, 2009, and 2012/13 experimental campaigns of AUG. In 2007-2009, the tiles were mounted in the divertor region while in 2012/13 they were located at the top of the vessel (upper divertor) and the inner heat shield. The poloidal locations of the tiles during each campaign are shown in Figure 1; in the case of heat-shield tiles also their positions in different toroidal sectors of AUG (out of 16) are indicated (top right).

In the divertor region, all the tiles had poloidal W marker stripes (thickness 200-1500nm) on fine-grained graphite [3] and an uncoated area for studying re-deposition of W. In addition, 1000-5000nm thick, poloidal Ni markers had been produced on the outer-divertor tiles. In the main chamber, most of the tiles were coated with poloidal (upper divertor) or toroidal (heat shield) W (thickness 1500nm) and Ni (thickness 2000nm) markers. In the heat-shield region, both W/Ni marker tiles and tiles with a 2-μm P92 steel coating – main components Fe, Cr (9.5wt.%), and W (2.0wt.%) – were used toroidally next to each other (see Figure 1); P92 was used because it was readily available and its composition and magnetic properties are similar to those of EUROFER [6].

The number of plasma shots and the divertor plasma time during each campaign are shown in Table 1. The auxiliary heating powers were rather similar in 2007-2009, on average 3-4MW, but a larger number of high-power shots (>8MW) could be carried out from 2008 onwards thanks to regular boronizations of the AUG vessel [8]. Under such conditions, power loads at the divertor increase by >50% [8], which is supported by the gradual increase of the measured divertor fluences (0.5×10^{26}m^{-2} in 2007, 1.6×10^{26}m^{-2} in 2009). The upper-divertor tiles were exposed during the first half of the 2012/13 campaign and the heat-shield tiles

during the entire campaign. Exceptions were the P92 tiles HS6, HS8, and HS12 from sector 1, which were in only during the second period.

The erosion/deposition profiles of the marker tiles were obtained by carrying out Rutherford Backscattering Spectroscopy (RBS) measurements before and after plasma exposure [9]. Protons with an energy of 2.5-3.0MeV were used in the analyses and the scattered particles were detected at 165°. The spectra were simulated using the SIMNRA code (see [9]). The accuracy for determining the thickness of a marker is ~3%, largely limited by inaccuracies in measuring the proton beam current.

2.2. Probe experiments

For the discharge-resolved experiments, two identical graphite probes were produced and coated with 50-100nm thick W, Ni, Al, and C (separated by a W interlayer) markers; here we focus on the W and Ni stripes. A photograph of one of the probes is inserted in Figure 1. The tip of the probes was tilted by 45° from the horizontal reference plane and positioned to face the magnetic field lines with magnetic connection towards the divertor. During the discharges, the tip of each probe was at a distance of 40-45mm outside the separatrix.

In the first experiment, one probe was exposed to L-mode shots in deuterium (AUG shot numbers #26725-26728). The plasma current was I_p=1MA, the toroidal field B_t=-2.8T, the line-averaged density n_e=6.2×10^{19}m^{-3}, and the auxiliary heating power P_{aux}=1.4MW. The overall exposure time was around 15s. The second probe was exposed to low-power H-mode discharges in deuterium (shots #29187-29190). The following parameters were used: I_p=0.6MA, B_t=-2.3T, n_e=5.3×10^{19}m^{-3}, P_{aux}=4.2MW, and total exposure time of ~25s.

Similarly to the marker tiles, RBS was used to extract the erosion/deposition profiles of the different marker stripes, this time using 2.0-MeV $^4He^+$ ions. Since the absolute erosion is only a few nanometers, the accuracy of the SIMNRA fittings becomes the limiting factor, resulting in a constant error of ~0.5nm.

3. Long-term erosion/deposition profiles in the AUG torus

3.1 Divertor region

The outer divertor of AUG is generally a net erosion and the inner divertor a net deposition region for W. This can be seen in Figure 2, where the poloidal profiles for the erosion/deposition rates of the W markers during the 2007, 2008, and 2009 experimental campaigns are presented; see [9] for the details of the 2007 data. Comparison between the different campaigns shows that net deposition in the inner divertor is the strongest in 2007 (up to 0.06nm/s) whereas in 2009 even small net erosion is locally observed. At the outer divertor, net erosion reaches its maximum (~0.12nm/s) close to the outer strike point (OSP) and then diminishes towards the main chamber. Interestingly, in 2008 net deposition dominates most of the outer-divertor PFCs in contrast to the situation in 2007 and 2009. This we attribute to enhanced main-chamber sources of W from 2008 onwards, which, however, are balanced by more intense erosion of PFCs as a result of impurity seeding experiments starting in 2009. Strong re-deposition of the eroded tungsten plays also a large role close to the OSP: according to Figure 2b, the re-deposition rate on graphite is 0.02-0.03nm/s.

By assuming erosion and deposition being toroidally symmetric, the integrated average mass gain of W at the inner divertor and roof baffle is 1.9mg/s. The corresponding value for the mass loss close to the OSP is 2.0mg/s and 1.0mg/s elsewhere at the outer divertor. The assumption of uniform erosion/deposition is supported by ASCOT simulations [12], which show the deposition patterns becoming toroidally symmetric almost everywhere in the torus. The overall picture is therefore that the eroded W is predominantly transported by the SOL plasma towards the inner parts of the AUG vessel.

In the case of Ni, the erosion profiles are qualitatively similar to those of tungsten but the absolute values are 5-10 times larger (see Figure 2c), in accordance with predictions in [10]. Around the OSP, almost all the original coating is gone, which corresponds to a large

mass-loss rate of 10mg/s, while further up on the outer-divertor PFCs, the rate is ~2.3mg/s. These values prove that steel is not a feasible PFC material in the divertor region.

3.2 Main chamber

In contrast to the lower divertor, the top of the AUG vessel is a strong net-deposition region for W. This becomes evident from Figure 3a where the poloidal erosion/deposition profiles of W at the upper divertor during the 2012/13 campaign are shown. Only at the outermost corner, small net erosion is observed but the error bars are relatively large. In addition, since there are strong W sources all over the torus, the intrinsic erosion/deposition patterns at the upper divertor are masked by the large influx of W from other regions of the AUG vessel. Besides, the deposits on PFCs mainly consist of H, D, B, and C, with deposition rates 1.5-7 times larger than that of W. Nevertheless, by assuming erosion and deposition being toroidally symmetric, the deposition rate at the top of the vessel becomes 0.05mg/s at the outer side and 0.9mg/s at the inner side.

In the heat-shield region, the W markers above and around the midplane show marginal net deposition of <0.003nm/s while below the midplane, the deposition turns into slightly larger net erosion (see Figure 3b). However, due to the noticeable error bars these values should be taken with caution. If we assume that the measured surface densities are representative also for the neighbouring tiles, we obtain after toroidal integration that the balance is slightly towards erosion, with the integrated mass-loss rate being 0.07mg/s.

Considering Ni and P92 steel, the situation is more complicated. According to Figure 3a, the upper divertor shows net erosion except for the immediate neighbourhood of the secondary X-point where erosion and deposition peaks alternate. Since the deposited Ni originates only from the immediate neighbourhood of the particular markers, PFCs at the top of the vessel would generally exhibit minor net erosion in the absence of divertor or main-chamber sources; in the case of Ni the toroidally integrated mass loss would be 0.3mg/s.

What comes to the heat shield, the Ni markers show net deposition everywhere else than at the midplane. The results, however, depend on the toroidal location of the PFCs: the tiles from sectors 2 and 7 indicate net erosion, the tiles from sector 12 net deposition. This could be due to local damages of the markers and accumulation of the eroded material on the surrounding areas, thus requiring a careful investigation of also the P92 tiles. Almost all these markers showed small but measurable net erosion. However, the data have mostly been gathered from sector 1, where neutral beam injection (NBI) shine-through regions exist. When moving to other sectors, the observed erosion rate of ~0.007-0.008nm/s on the P92 tiles below HS6 turns into very small deposition of <0.001nm/s. The toroidally integrated mass-loss rate would thus be around 0.2-0.4mg/s, which is 3-5 times larger than the corresponding erosion rate for W. Again due to the considerable error bars, the values above are only indicative and the observed net erosion may even turn out to be marginal net deposition. This could be possible since the tiles contained an up to 1-μm thick boron-rich surface layer.

As a conclusion, the inner column is a small source of impurities into the plasma even though under non-boronized conditions this region has been noticed to be the dominant main-chamber W source [7]. Erosion is also an issue at the upper divertor, at least in the case of Ni or steel. Nevertheless, steel could be used in these regions in the form of marker coatings: The expected erosion, e.g., during the 2012/13 campaign is below 100nm.

4. Discharge-resolved erosion/deposition profiles at the outer midplane

Based on the probe data, the outer midplane is a noticeable net-erosion region for W and Ni as Figure 4 shows. In the case of W, the net-erosion rate around the limiter PFCs is about 0.05nm/s but due to large error bars, the real values are between 0 and 0.1nm/s. As expected, the erosion peaks close to the probe tip and then decays towards the limiters. The average electron temperature (T_e) of the SOL plasma was lower during the H-mode than the

L-mode experiment, which could explain why the observed erosion is smaller during the H-mode shots.

In the case of Ni, the erosion profiles resemble those of W but the measured values are again 5-10 times higher: the determined erosion rates are 0.4-0.8nm/s. As a result, during the 2012/13 campaign tungsten would experience net erosion of <1 μm and steel 4-6μm. These estimates are, however, not the whole truth since (i) the outer midplane of AUG consists of discrete sets of limiter tiles (total area ~25000cm^2) and (ii) the same particle flux that hits a single probe would be distributed on all the limiter components. On the other hand, no ICRF heating was used in these experiments, which is known to locally increase W influx from antenna limiters [7]. In any case, the outer midplane contributes significantly to the release of W in the SOL plasma, with the values above the mass-loss rate would be 2.4mg/s.

5. Conclusions

In this article, we have experimentally studied net erosion/deposition profiles of W and steel (or Ni) in different regions of the AUG torus during its full-W operational phase. The inner divertor is a net deposition and the outer divertor a net erosion region of W, with some 20-25% of the eroded W being re-deposited on close-by surfaces. During long-term operations, the inner heat shield is a small and the outer midplane a major net-erosion region for W, and of the eroded W some 40-60% ends up in the inner divertor and 20-30% at the top of the vessel. The remaining W is deposited in shadowed areas of the tokamak.

Considering steel and Ni, they are eroded 3-10 times faster than W leading to unacceptably high erosion yields at the outer divertor and at the outer midplane. From the erosion point of view, under standard, lower single-null discharges steel could be used at the upper and inner parts of the main chamber where the mass-loss rate is 0.01-0.05nm/s.

Presently, ERO [11] simulations are ongoing to explain the physics behind erosion at the outer midplane. Preliminary results suggest a good match between simulations and

experimental results when using relatively long decay lengths for the SOL plasma parameters (30-40mm), especially for the electron and ion temperatures. ELMs have been observed to dominate erosion if their share of the total simulation time is at least 20%, and generally the ELM-induced erosion is only affected by the total duration of the ELMs.

Acknowledgments

This project has received funding from Tekes – Finnish Funding Agency for Technology and Innovation – and the European Union's Horizon 2020 research and innovation programme. The views and opinions expressed herein do not necessarily reflect those of the European Commission

References

[1] R. Neu et al., Plasma Phys. Control. Fusion 53 (2011) 124040.

[2] M. Rubel et al., J. Nucl. Mater. 438 (2013) S1204.

[3] R. Neu et al., Phys. Scr. T138 (2009) 014038.

[4] V. Philipps, J. Nucl. Mater. 415 (2011) S2.

[5] H. Bolt et al., J. Nucl. Mater. 307-311 (2002) 43.

[6] H. Neuberger et al., Fusion Eng. Des. 86 (2011) 2039.

[7] R. Dux et al., J. Nucl. Mater., 390-391 (2009) 858.

[8] A. Kallenbach et al., Nucl. Fusion 49 (2009) 045007.

[9] M. Mayer et al., Phys. Scr. T138 (2009) 014039.

[10] R. Behrisch and W. Eckstein (Eds.), Sputtering by Particle Bombardment, Topics in Applied Physics 110, Springer, Berlin, 2007.

[11] A. Kirschner et al., Nucl. Fusion 40 (2000) 989.

[12] J. Miettunen et al., Nucl. Fusion 52 (2012) 032001.

Table 1. Number of discharges and plasma time during the experimental campaigns 2007, 2008, 2009, and 2012/13.

Campaign	Number of discharges	Divertor plasma time (s)
2007	605	2621.4
2008	726	3529.3
2009	1101	5274.5
2012/13, 1st half	1106	4747.1
2012/13, 2nd half	1611	6609.4

Figure captions

Figure 1. Poloidal and toroidal (heat-shield tiles) locations of marker tiles removed from AUG for surface analyses after different campaigns. The inset shows a photograph of one erosion probe. The arrows indicate the direction of the poloidal *s* coordinate.

Figure 2. (a) Erosion/deposition profiles for W markers in the inner divertor. (b) Correponding profiles in the outer divertor, including re-deposition graphs for W on graphite. (c) Erosion/deposition profiles for Ni markers in the outer divertor. Negative values indicate net erosion, positive values net deposition.

Figure 3. (a) Erosion/deposition profiles for W and Ni markers in the upper divertor. (b) Toroidally averaged erosion/deposition data for W, Ni, and P92 markers in the heat shield.

Figure 4. Erosion/deposition profiles for (a) W and (b) Ni along the markers on erosion probes during L- and H-mode experiments.

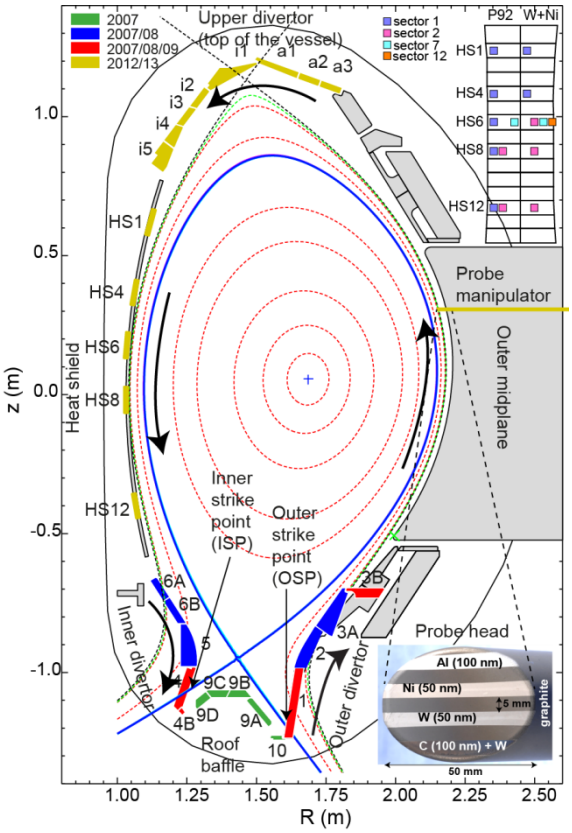
2007
2007/08
2007/08/09
2012/13
Upper divertor
(top of the vessel)
sector 1
sector 2
sector 7
sector 12
P92
W+Ni
HS1
HS4
HS6
HS8
HS12
i1
i2
i3
i4
i5
a1
a2
a3
Probe
manipulator
Outer midplane
Heat shield
Inner
strike
point
(ISP)
Outer
strike
point
(OSP)
6A
6B
5
9C
9B
4B
9D
9A
Roof
baffle
10
1
2
3A
3B
Inner divertor
Outer divertor
Probe head
Al (100 nm)
Ni (50 nm)
W (50 nm)
C (100 nm) + W
5 mm
graphite
50 mm
z (m)
R (m)
1.0
0.5
0.0
-0.5
-1.0
1.00
1.25
1.50
1.75
2.00
2.25
2.50

Figure 1

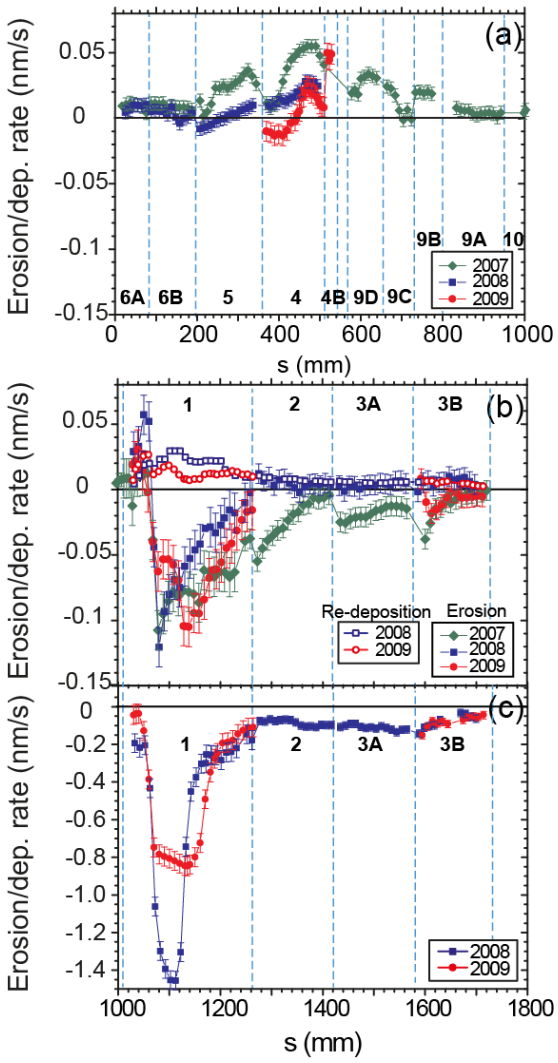
(a)
Erosion/dep. rate (nm/s)
0.05
0
-0.05
-0.1
-0.15
0
200
400
600
800
1000
s (mm)
6A
6B
5
4
4B
9D
9C
9B
9A
10
2007
2008
2009
(b)
1
2
3A
3B
Re-deposition
Erosion
2008
2009
2007
2008
2009
(c)
0
-0.2
-0.4
-0.6
-0.8
-1.0
-1.2
-1.4
1000
1200
1400
1600
1800
s (mm)
1
2
3A
3B
2008
2009

Figure 2

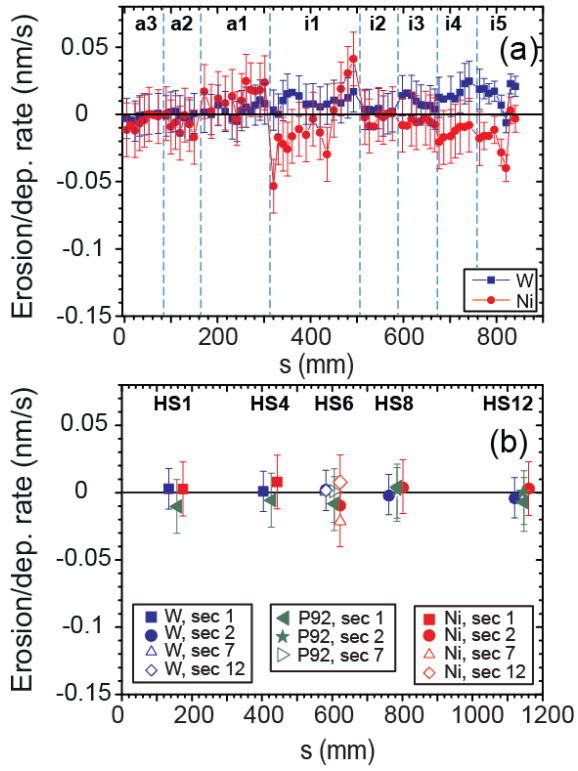
a3
a2
a1
i1
i2
i3
i4
i5
(a)
Erosion/dep. rate (nm/s)
0.05
0
-0.05
-0.1
-0.15
0
200
400
600
800
s (mm)
W
Ni
HS1
HS4
HS6
HS8
HS12
(b)
W, sec 1
W, sec 2
W, sec 7
W, sec 12
P92, sec 1
P92, sec 2
P92, sec 7
Ni, sec 1
Ni, sec 2
Ni, sec 7
Ni, sec 12
1000
1200

Figure 3

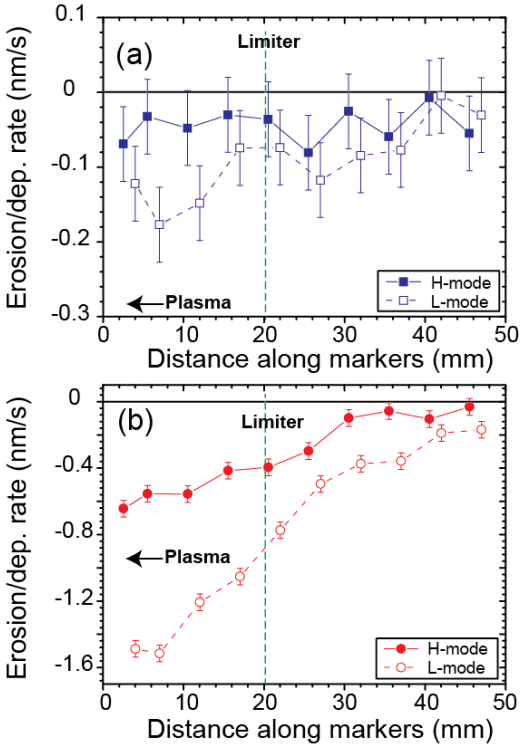
(a)
Limiter
Plasma
H-mode
L-mode
Erosion/dep. rate (nm/s)
Distance along markers (mm)
(b)
Limiter
Plasma
H-mode
L-mode
Erosion/dep. rate (nm/s)
Distance along markers (mm)

Figure 4